Journal of Materials Chemistry A

Accepted Manuscript

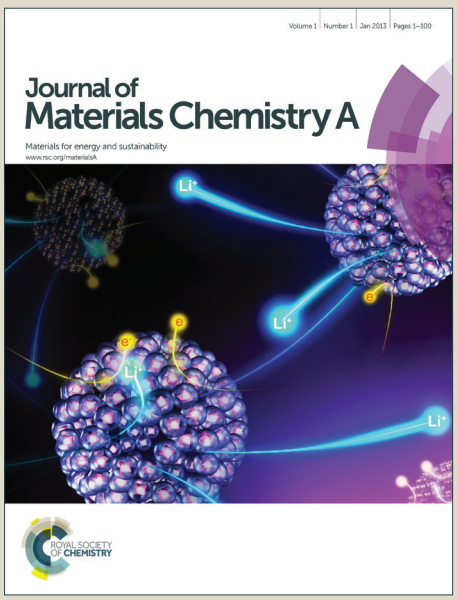

ROYAL SOCIETY OF CHEMISTRY

www.rsc.org/materialsA

Journal of Materials Chemistry A

Cite this: DOI: 10.1039/c0xx00000x

ARTICLE TYPE

www.rsc.org/xxxxxx

Enabling a High Capacity and Long Cycle Life of Nano-Si Anode by Building a Stable Solid Interface with Li^+-Conducting Polymer

Shi Zeng[a], Daotan Liu[b], Yao Chen[a], Jiangfeng Qian[a], Yuliang Cao[a], Hanxi Yang[a], Xinping Ai[a]*

Received (in XXX, XXX) Xth XXXXXXXXX 20XX, Accepted Xth XXXXXXXXX 20XX

DOI: 10.1039/b000000x

Great efforts have been devoted to develop nano-Si anode for next-generation lithium ion batteries (LIBs); however, all the Si anodes developed so far still need to improve their reversible capacity and cycling stability for battery applications. In this work, we propose a new strategy to develop cycling-stable Si anode by embedding nano-Si particles into a Li^+-conductive polymer matrix, in which a stable Si/polymer interface is established to avoid the contact of Si surface with electrolyte and to buffer the volume change of the Si lattice during cycles, thus promoting the capacity utilization and long cycle life of nano-Si particles. The nano-Si/polybithiophene composite synthesized in this work demonstrates a high Li-storage capacity of >2900 mA h g^{-1}, a high-rate capability at 12 A g^{-1} and a long-term cyclability with >1000 mA h g^{-1} over 1000 cycles, possibly serving as a high capacity anode for lithium battery applications. In addition, the fabrication technique for this type of composite material is facile, scalable and easily extendable to other Li-storable metals or alloys, opening up a new avenue for developing high capacity and cycle-stable anodes of advanced Li-ion batteries.

Introduction

Advanced lithium ion batteries (LIBs) with higher safety and higher capacity are actively developed in the past decade as a promising power source for electric storage applications ranging from portable electronics, electric vehicles to smart grids.[1-3] One of the critical challenges in this technology development is to find safer and higher capacity alternatives for replacement of the carbonaceous anodes currently used in Li ion batteries. Among the possible alternative anodes, Si is far ahead of other Li-storable metals and alloys with an exceptionally high gravimetric capacity (4200 mA h g^{-1}, $Li_{4.4}Si$) and a considerably safer lithiation potential (+ 0.2 V, vs Li^+/Li).[4] However, the battery application of Si anode is still limited by its poor cyclability due to the huge volume change (~ 400%) arising from the formation of various Li_xSi phases.[5-7] Such a volume change can produce a huge mechanical stress, leading to the continuous pulverization and electric disconnection of Si particles. Another severe but often ignored problem brought about by the large volume change is the continuous reconstruction of the solid electrolyte interphase (SEI) on the Si surfaces, which ceaselessly consumes Li ions and electrolyte, leading to a low current efficiency and continuous capacity degradation of the Si anode during cycling.[8, 9]

To alleviate these problems, various strategies have been proposed to buffer the volume change by use of nanosized Si particles,[10] inactive/active composites,[11, 12] ultrathin film electrodes[13] and porous Si nanoarchitecture,[14, 15] so as to enhance the structural stability and the cycling performance of Si anodes. Despite a number of the nano-Si anodes have demonstrated considerably high capacities and strong cyclability in Li half cells.[16-19] Their battery applications are less successful because of the fact that there is not an enough amount of Li ions and electrolyte affordable for the repeated destruction/reconstruction of the SEI films on the Si surfaces in practical batteries.

Building a protective coating on Si anodes to avoid the direct contact of Si particles with liquid electrolyte seems to be a simple way for establishing stable Si surfaces. Many attempts have been made to coat the nano-Si particles with multilayer graphene,[20] amorphous carbons[21] and Li-storable metals[22] to block off the impact of electrolyte; however, these coatings are easily fractured at the repeated expansion/contraction, losing their ability to protect the Si surfaces unattacked at charge-discharge cycling. Though conductive polymers may offer a flexible surface coating for accommodating the large volume changes of Si anodes, the stretch and shrinkage of such non-selective polymer coatings can also allow the electrolyte to pass through, leading to an imperfect shielding of the nano-Si surfaces. Our recent work has demonstrated that nano-Si particles could be well cycled to remain a high reversible capacity of >1600 mA h g^{-1} over 400 cycles when they were deeply embedded in Li^+-conductive polyparaphenylene (PPP).[23] Moreover, Cui et al recently reported a yolk-shell structured Si/C composite with rationally designed void space, which showed a reversible capacity of 1000 mAh g^{-1} at 1C rate over 1000 cycles, due to the strong buffering effect of the local void space for the large volume change, thus stabilizing the interfacial structure of the nano-Si particles.[24]

Combining the advantages offered by both the conductive polymer coating and the hollowed nanostructure on the electrode materials, we attempted to construct a core-shelled nano-Si/polybithiophene composite (Si/PBT) with self-formed nano-voids, where nano-Si cores act as an active Li-storage phase, while the conducting polymer matrix serves not only as conductive channels for electron and Li ions, but also as a protective barrier to prevent the direct contact of the Si surface with electrolyte. More significantly, the flexible polymer matrix can create a nanovoid around each Si particle due to the volume expansion/contraction of the Si cores during initial charge/discharge cycles, thus providing a further buffering action. Benefiting from the stable solid interface and flexible buffer matrix formed by Li-conducting polymer, this Si/PBT material can not only give a very high Li-storage capacity of > 2900 mA h g^{-1} at a constant current of 300 mA g^{-1}, but also an enhanced cyclability with 1000 mA h g^{-1} delivered at a high rate of 3 A g^{-1} over 1000 cycles. Particularly, the synthetic approach to the Si/PBT material is simple, scalable and emission- free, possibly applicable to other Li-storable metals and metalloids for creating high performance alternative anodes for a new generation of Li-ion batteries.

Experimental

Materials synthesis

PBT was synthesized by oxidative polymerization of bithiophene monomer in chloroform solution with $FeCl_3$ as oxidant.[25] A detailed synthetic procedure was as follows: 0.168g (1 mmol) bithiophene (Alfa Asear) was dissolved in 4 mL chloroform under nitrogen atmosphere. 0.648 g (4 mmol) $FeCl_3$ was divided into four equivalent portions and then added severally into the reaction solution at an interval of 1 h. The reaction mixture was stirred under nitrogen atmosphere for 24 h and then poured into methanol for precipitating out the polymer product. The polymer precipitate was collected and washed several times with methanol, and then, the collected polymer powders were purified by Soxhlet extraction. Finally, the polymer product was dried in vacuum at 50 ºC for 12 h. Nano-Silicon/polymer composite were prepared simply by ball-milling silicon nanoparticles (less than 100 nm, Alfa Aesar) with the synthesized PBT at a weight ratio of 5:2 for 30 min. The ball milling was conducted in a planetary ball mill (Fritsch pulverisette 23) under Ar atmosphere.

Structural characterizations

The FT-IR spectra of Si/PBT composite were recorded on a NICOLET AVATAR360 FT-IR spectrometer with KBr pellets. The morphological and structural characteristics of the as-prepared powder samples were examined by scanning electron microscope (SEM, JEOL, JSM-6700F) operating at 10KV and transmission electron microscopy (TEM, JEOL, JEM-2010-FEF) operating at an accelerating voltage of 200 kV, respectively.

Electrochemical measurements

CR2016-type coin cells with Celgard 2400 microporous membrane as separator and lithium disk as counter electrode were assembled in an argon-filled glove box for all electrochemical characterizations. The electrolyte used in this work was 1 M $LiPF_6$ dissolved in a mixture of ethylene carbonate (EC), dimethyl carbonate (DMC) and ethyl methyl carbonate (EMC) (1:1:1 in volume ratio, Shinestar Battery Materials Co., Ltd., China). The composite silicon anodes were prepared by casting the electrode slurry onto a 20 μm thick copper foil. The electrode slurry was composed of silicon/polymer composite, Ketjen Black and polyacrylic acid (PAA) binder with a wt.% ratio of 70%-10%-20%, dissolved in distilled water. The contents of nano-Si and PBT polymer in the as-prepared composite anode are 50 wt.% and 20 wt.%, respectively. The electrodes were dried at 60 ºC under a vacuum for overnight to remove the water. The mass loading of nano-Si in the electrode is 1.6 mg cm^{-2}.For comparison, the pristine nano-silicon anode was also prepared in the similar way with a composition of 50 wt.% nano-silicon powders, 30wt.% Ketjen Black and 20 wt.% PAA binder. The PAA binder used in this study has an average molecule weight of 240000 g/mol, purchase from Alfa Asear. The charge/discharge experiments were performed on Land Battery Testing System (Wuhan Kingnuo Electronics Co., Ltd., China) at 25 ºC. The cutoff voltage is 0.01 V versus Li/Li^+ for discharge (Li insertion) and 2.0 V versus Li/Li^+ for charge (Li extraction). Cyclic voltammetry (CV) was performed on an electrochemical workstation (CHI660c, Shanghai, China) in a voltage range of 0.005-2.0 V at a scan rate of 0.1 mV s^{-1}. The electrochemical impedance measurement was conducted on an Impedance Measuring Unit (IM 6e, Zahner) with oscillation amplitude of 5 mV over the frequency range from 50 mHz to 100 kHz.

Results and Discussion

The Si/PBT composite was synthesized simply by ball-milling commercial silicon nanoparticles (less than 100 nm in diameter) with PBT at an optimized Si/PBT ratio of 5:2 (by wt.) for 30 min. Detailed preparation processes are described in the experimental section. Ball milling method was chosen to embed Si nanoparticles in a PBT matrix because of its simplicity to enable a uniform dispersion of rigid nanoparticles in ductile polymers, as used frequently in the previous fabrication of a large range of polymer nanocomposites such as nanofiber-strengthened polymers and nano-alloy/polymer composites.[26-29]

Fig. 1a shows the morphological feature of the Si/PBT composite. The TEM image clearly reveals that the Si/PBT composite has a core-shelled structure with sphere-like nanoparticles (strong contrast) embedded in a polymer matrix (weak contrast). The electron diffraction image from an embedded nanoparticle in Fig. 1b shows a cubic symmetry diffraction spot pattern, indicating a crystalline Si phase. Exclusively, the amorphous matrix must be given by PBT polymer. High-resolution TEM image from a single grain boundary in Fig. 1c confirms that the Si nanoparticle is compactly coated with a dense PBT polymer. It is just this polymer matrix that separates Si cores with electrolyte. The infrared spectrum of the as-prepared composite sample shows clearly all the strong characteristic vibrations of PBT polymer only (Supporting information, Fig. S1), demonstrating that the Si particles were deeply embedded within the PBT matrix. This can also be evidenced by the morphological changes of PBT polymer before and after ball milling. As reflected by the SEM images in Fig. S2, the pure PBT polymer is a flake-like aggregate with smooth surfaces. After ball-milled with nano-Si particles, the

polymer surface became much rougher. Undoubtedly, this roughness is caused by the inserting of Si nanoparticles into the polymer matrix.

The formation processes of the Si/PBT composite are schematically illustrated in Fig. 1d. At the initial stage of milling, the ductile PBT powders are unfolded at the impact of milling balls with the nano-Si particles wrapped in the polymer fibers. During the repeated folding and unfolding processes enforced by ball-milling, the nano-Si particles are gradually embedded into the bulk phase of the PBT polymer. Furthermore, the vigorous ball-powder-ball collisions promote the uniform dispersion of nano-Si in the polymer matrix.

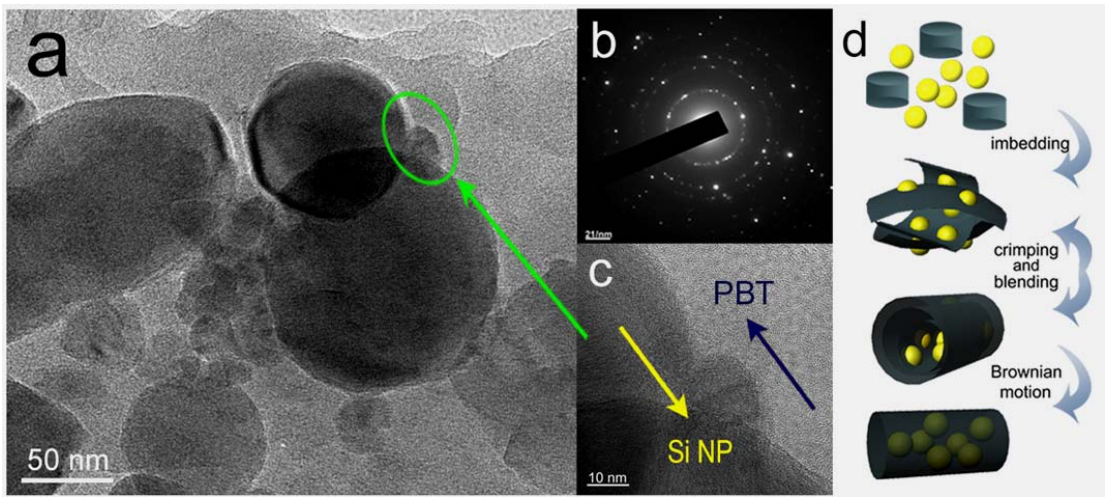

Fig. 1 a) TEM image, b) Electron diffraction patteren, and c) HRTEM image of the Si/PBT composite, d) Schematic illustration of the formation processes of the core-shelled Si/PBT composite during ball milling.

The electrochemical Li-storage properties of the Si/PBT composite were characterized by cyclic voltammetry (CV) and galvanostatic charge-discharge measurements. As observed from the CV curves in Fig. 2a, the Si/PBT electrode displays a very weak and broad reduction band in the initial cathodic scan from 1.0 V to 0.3 V, indicating that the decomposition of electrolyte for building SEI film is greatly suppressed, unlike the huge irreversible cathodic bands usually observed from Si surfaces.[30-32] This CV feature further confirms the blocking effect of the polymer matrix on the soakage of electrolyte. At subsequent scans, two pairs of strong cathodic/anodic peaks appear at 0.2/0.52 V and 0.08/0.35 V, respectively, characterizing the reversible Li alloying/dealloying reactions on the Si/PBT composite. These CV peaks resemble very much those observed from pristine Si/C anodes in the peak shapes and potential positions,[33, 34] suggesting that the PBT polymer matrix did not block off the Li^+ transport into and Li^+-alloying with the Si nanoparticles.

Fig. 2b displays the initial charge-discharge profiles of the Si/PBT composite at a constant current of 300 mA g^{-1}. The initial charge and discharge capacities are 4200 mA h g^{-1} and 3095 mA h g^{-1}, respectively, corresponding to a ~75% capacity utilization of the highest theoretical 4.4 Li-storage reaction of Si. Also, the initial coulombic efficiency of this material at first cycle attains to 74%, considerably higher than the values reported from the carbon-coated nano-Si anodes. The high capacity utilization and initial coulombic efficiency of the Si/PBT composite imply that the PBT matrix can not only effectively protect the Si surface from the etching of electrolyte but also promote the Li-alloying reaction with Si phase. Although the reversible capacity is sufficiently high, there still exists a large irreversible capacity of ~ 1105 mA h g^{-1} in the first cycle. Except for the irreversible insertion of Li ions in PBT matrix, the irreversible capacity is also related to the formation of SEI film on the surface of Si/PBT composite. To improve the initial Coulombic efficiency, a possible way is to choose suitable film-forming additives for the Si/PBT composite, so as to reduce the first irreversible capacity loss. Some additives, such as vinylene carbonate (VC), vinylethylene carbonate (VEC) and lithium bis(oxalato) borate (LiBOB) are being investigated for this purpose in our lab.

The most important advantage offered by the PBT matrix is the establishment of a solid/solid interface between the Si nanocores and their polymer surroundings, which are expected to promote the cycling performance of the Si/PBT anode. To obtain a direct evidence for the improved cyclability, we cycled for comparison the Si/PBT anode and the pristine nano-Si anodes in Li-half cells at the same conditions. As shown in Fig. 2c, although the nano-Si anode can delivers a quite high capacity of 2490 mA h g^{-1} at the first cycle, its reversible capacity decreases rapidly down to 600 mA h g^{-1} in the first 100 cycles, then continuously declines to 300 mA h g^{-1} in the subsequent 100 cycles, corresponding to a capacity retention of 10 % at the 200th cycle. In contrast, the Si/PBT anode exhibits a greatly improved cycling stability. Except for a high initial capacity of 2960 mA h g^{-1}, the Si/PBT anode delivers a reversible capacity of up to 1500 mA h g^{-1} at the 300th cycle and 1350 mA h g^{-1} at the 500th cycle. Even after 1000 cycles, the reversible capacity can still keep at ~ 1000 mA h g^{-1}. To the best of our knowledge, such a superior long-term

cyclability is rarely reported for the Si-based anodes.[35-37] This excellent cyclability must be associated with a stable high charge/discharge efficiency of the Si/PBT anode during prolonged cycling. As also displayed in Fig. 2c, the average Coulombic efficiency keeps at ~99.72% from the 100th to the 1000th cycles, suggesting that the inner Si/PBT interface and the outer PBT/electrolyte interface remain stable during cycling, avoiding the reconstruction process of the SEI film usually encountered in conventional Si anodes.

Based on the quite high Coulombic efficiency of the Si/PBT anode during cycling, we assembled a coin-type full cell using the Si/PBT as anode and $LiCo_{1/3}Ni_{1/3}Mn_{1/3}O_2$ (NCM) as cathode and tested the cells by galvanostatic charge and discharge cycling. Since the specific capacity of the Si/PBT anode is ten times higher than that of NCM cathode, the cells have to be assembled with an anode limited design and therefore the reversible capacity of the cell is actually determined by the mass of anode material. Fig.S3 display the charge–discharge curves and cycling performance of such full cells. Similarly like in the case of Li half cells, the Si/PBT electrode demonstrated charge/discharge capacities of 3600/2600 mA h g^{-1} in the first cycle with a Coulombic efficiency of ~ 72%. The reversible capacity of the Si/PBT composite in the full cells gradually decreased from 2600 to 1620 mAh g^{-1} after 100 cycles, exhibiting a considerable cyclability as an acitive anode material.

The stability of the SEI film is also confirmed by the electrochemical impedance spectra (EIS) and XPS spectra of the Si/PBT electrode at different cycles. As shown in Fig. S4, the diameter of the semi-circle at the high frequency region, representing the impedance of SEI film, almost remains unchanged during cycling. Fig.S5 show the XPS spectra collected from the surface of Si/PBT electrode at different cycles. As can be seen in Fig. S5, the XPS spectra of C 1S and O 1S, characterizing the surface properties of Si/PBT electrode, almost remains unchanged as the cycles increase from 10 to 50, indicating the high stability of SEI film.

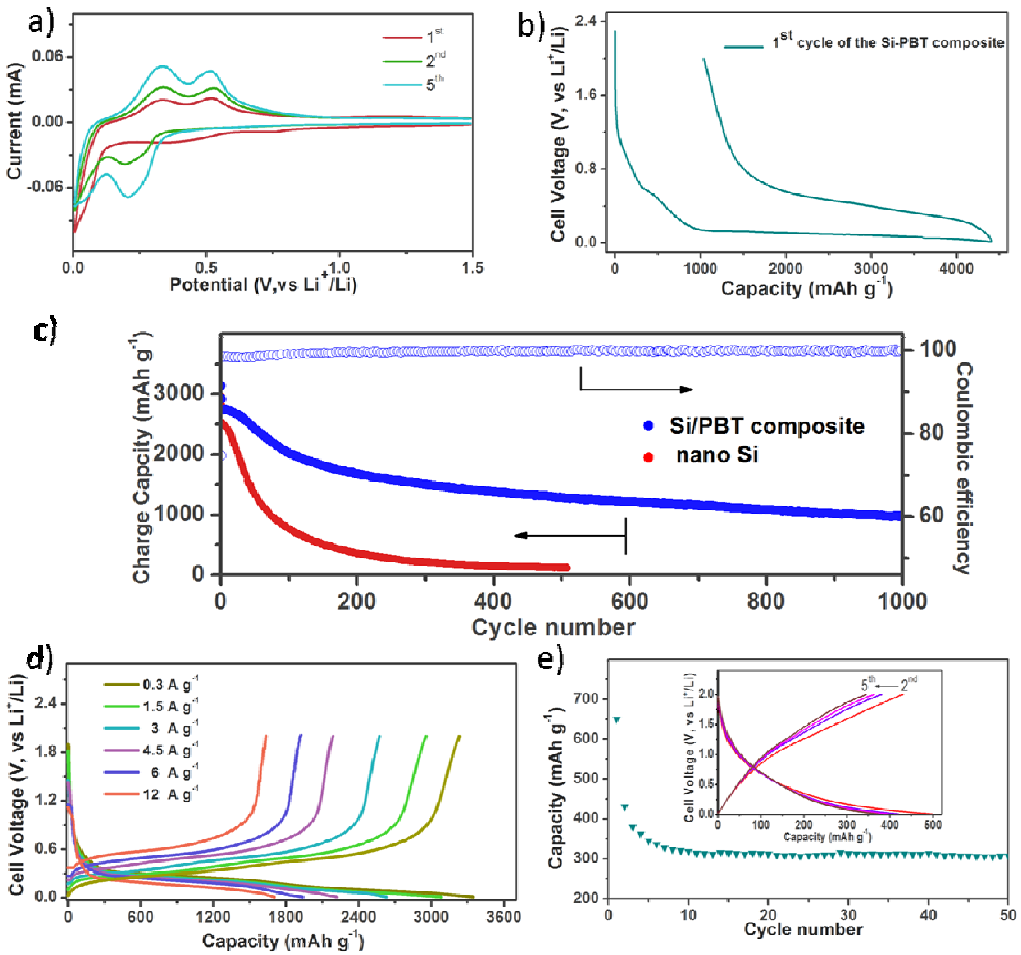

Fig.2 a) CV curves of the Si/PBT composite electrode at a scan rate of 0.1 mV s^{-1}; b) charge-discharge curves of the Si/PBT composite electrode between 0.01 V - 2.0 V at a current of 300 mA g^{-1}; c) cycling performance of the pristine nano-silicon and Si/PBT composite electrodes. All the electrodes were cycled at 300 mA g^{-1} for the first cycle, 1500 mA g^{-1} for the second cycle, and 3000 mA g^{-1} for the later cycles; d) charge-discharge curves of the Si/PBT composite electrode at various currents from 300 mA g^{-1} to 12 A g^{-1}; e) charge-discharge curves and cycling performance of the PBT electrode at a current density of 100 mA g^{-1}. The theoretical capacity of Si anode is 3570 mAh g^{-1} at room temperature and the reversible capacity of the pristine PBT electrode is ~ 325 mA h g^{-1}. According to the mass ratio of nano-Si to PBT polymer = 5:2 in the composite, 1C rate corresponds to a current density of 2643 mA g^{-1} for the nano-Si/PBT composite.

In addition to the high capacity and strong cyclability, the Si/PBT also demonstrates a high rate capability. As shown in Fig.

2d, the Si/PBT anode delivers a reversible capacity of 3233 mA h g^{-1} at 300 mA g^{-1}, 2957 mAh g^{-1} at 1.5 A g^{-1} and 2574 mA h g^{-1} at 3.0 A g^{-1}. Even at very high rates of 6 A g^{-1} and 12 A g^{-1}, this material can still deliver considerably high reversible capacities of 1924 mA h g^{-1} and 1636 mA h g^{-1}, respectively. This excellent rate capability suggests that the PBT matrix can not only provide sufficient electronic and Li^+ conductions into but also a facile interfacial charge transfer at the surface of the embedded Si particles. To obtain a direct evidence for the Li^+-conduction in the PBT matrix, we tested the Li^+-insertion behavior of pristine PBT electrode in 1 M $LiPF_6$/EC + DMC + EMC electrolyte. As displayed in Fig. 2e, the PBT electrode demonstrates a reversible charge/discharge bahavior with a stable capacity of ~ 325 mA h g^{-1} at a low potential region of 2.0 ~ 0.0 V. Over 50 cycles, the PBT electrode can still deliver a reverisble capacity of 310 mAh g^{-1} with stable cycling performance. As is well known, PBT is a bipolar conducting polymer with n-type redox activity,[38] which undergo redox reaction through reversible n-doping/dedoping processes accompanying with the reversible insertion of Li^+ ions in the polymer backbones for charge counterbalance. It is such a Li^+- doping reaction in the PBT polymer that provides sufficient amount of Li^+ ions for the further lithiation/de-lithiation reactions of Si nanoparticles.

To determine the migration rate of Li^+ ions in the PBT matrix, the diffusion coefficients of Li^+ ions were evaluated by electrochemical impedance spectra (EIS) of the PBT electrodes at different depths of discharge. Derived from the $Zre \sim \omega^{-0.5}$ plot of the EIS spectra (Fig. S6), the Li^+ diffusion coefficients in the PBT matrix were found to be in the amplitude of $1\sim10\times10^{-9}$ cm^2 S^{-1} as listed in Table S1, which are much higher than those reported for Si lattice (50 nm Si particles, 10^{-10} to 10^{-11} cm^2 S^{-1} [39]). With such a high conductivity, Li^+ ions can pass easily through the PBT matrix to arrive at the embedded Si particles without much kinetic frustration, therefore ensuring the high-rate capability of the Si/PBT composite.

To get a deep understanding of the mechanism for the stable cyclability, the microstructural evolution of the cycled Si/PBT anode was characterized by TEM technique. As seen in Fig. 3a, the Si nanoparticles contacts compactly with their PBT surroundings at charged state due to the volume expansion of the lithiated Si particles. When the electrode was discharged to extract out Li ions from the Si phase (Fig. 3b), there appears a void space around each Si nanoparticle due to the volume contraction of the Si lattice. Fig. 3c illustrates the formation process of the nanovoids in the Si/PBT anode during charge/discharge cycles. Such self-formed nanovoids resulting from the structural self-adjustment of the PBT matrix provide an additional buffer for accommodating the volume change of Si nanocores and stabilize the structural integrity of the PBT matrix, thus enabling a stable Si/PBT interface for the electrochemical Li-storage reaction during the prolonged cycles.

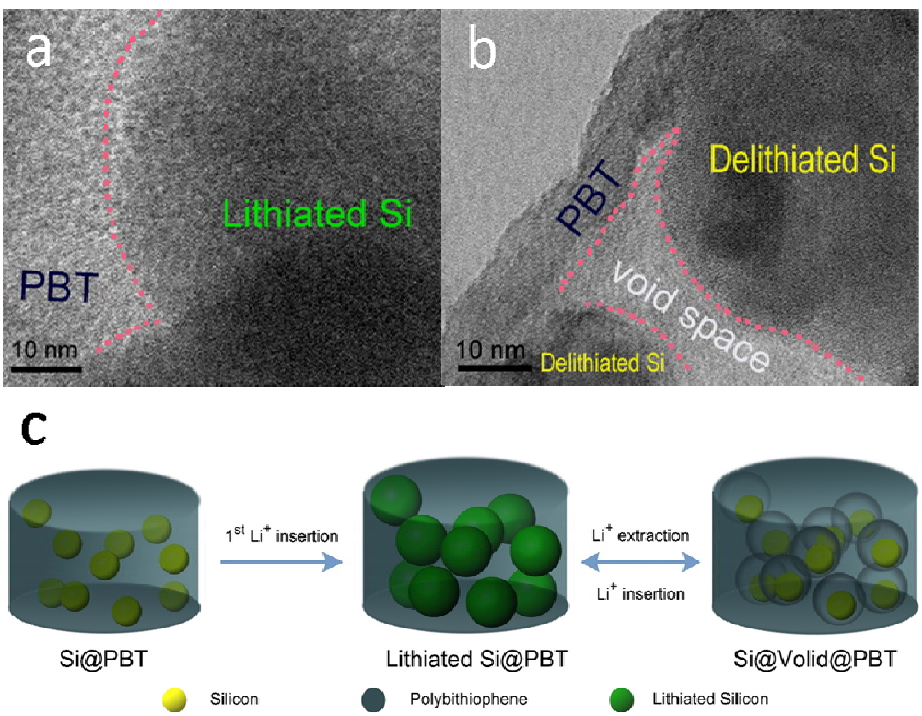

Fig.3 a) TEM image of the Si/PBT composite after the first lithiation; b) TEM image of the Si/PBT composite after the first delithiation; c) Schematic illustration of the structural evolution of conductive polymer-embedded nano-Si composite during lithiation and delithiation processes.

Conclusions

In summary, we demonstrate a new strategy to enhance the reversible capacity and long-term cycleability of Si particles by

embedding them in a Li^+-conductive polymer matrix, thus preventing the contact of the nano-Si surface with electrolyte and therefore avoiding the repeated construction of SEI film on the Si surfaces at cycling. The thus-prepared Si/PBT composite demonstrated a high Li-storage capacity of > 2900 mA h g^{-1}, a high rate capability of 12 A g^{-1} and a long-term cyclability with a capacity retention of > 1000 mA h g^{-1} over 1000 cycles at a very high rate of 3 A g^{-1}, showing a great prospect for battery application. Furthermore, the structural design and manufacture method for the nano-Si/polymer composites are facile and easily extendable to other Li-storable metals or alloys for developing high capacity and cycle-stable anode for next generation Li-ion batteries. However, it should be pointed out that embedding nano-Si particles within a polymer matrix will lead to a slight decrease in the density of the Si-based anode, which would produce negative impact on volumetric energy density of the cells.

Acknowledgements

This work was financially supported by the National High-tech R&D Program of China (2012AA052201), the National Science Foundation of China (21373154) and the 973 Program of China (No. 2015CB251100) .

Notes and references

[a] *Hubei Key Lab. of Electrochemical Power Sources, College of Chemistry & Molecule science, Wuhan university, Wuhan, 430072, China. Fax: +86-27-87884476; Tel: +86-27-68754526; E-mail: xpai @whu.edu.cn*

[b] *China Electric Power Research Institute, Beijing, 100192, China. Fax: +86-10-62913126; Tel: +86-10-82812114; E-mail: liudaotan@epri.sgcc.com.cn*

† Electronic Supplementary Information (ESI) available: FTIR spectra of the Si/PBT composite, SEM images of PBT and the Si/PBT composite, charge-discharge profile and cycling performance of the coin-type full cells using the Si/PBT as anode and NCM as cathode, the electrochemical impedance spectra (EIS) of the Si/PBT electrode at different cycles, XPS spectra of C 1S and O 1S collected from the surface of Si/PBT electrode at different cycles, the EIS spectra of the PBT electrode at different charge/discharge states, the relationship between Z_{re} and $\omega^{-0.5}$ at low frequency region, and the diffusion coefficient of Li^+ ion in the PBT electrode at different charge/discharge states. See DOI: 10.1039/b000000x/

1. R. Marom, S. F. Amalraj, N. Leifer, D. Jacob and D. Aurbach, *J. Mater. Chem.*, 2011, **21**, 9938-9954.
2. J. B. Goodenough and Y. Kim, *Chem. Mater.*, 2010, **22**, 587-603.
3. H. Li, Z. X. Wang, L. Q. Chen and X. J. Huang, *Adv. Mater.*, 2009, **21**, 4593-4607.
4. M. T. McDowell, S. W. Lee, W. D. Nix and Y. Cui, *Adv. Mater.*, 2013, **25**, 4966-4985.
5. X. H. Liu, L. Zhong, S. Huang, S. X. Mao, T. Zhu and J. Y. Huang, *ACS Nano*, 2012, **6**, 1522-1531.
6. U. Kasavajjula, C. S. Wang and A. J. Appleby, *J. Power Sources*, 2007, **163**, 1003-1039.
7. X. H. Liu and J. Y. Huang, *Energy Environ. Sci.*, 2011, **4**, 3844-3860.
8. H. Wu and Y. Cui, *Nano Today*, 2012, **7**, 414-429.
9. Y. Oumellal, N. Delpuech, D. Mazouzi, N. Dupre, J. Gaubicher, P. Moreau, P. Soudan, B. Lestriez and D. Guyomard, *J. Mater. Chem.*, 2011, **21**, 6201-6208.
10. J. Graetz, C. C. Ahn, R. Yazami and B. Fultz, *Electrochem. Solid-State Lett.*, 2003, **6**, A194-A197.
11. B.-C. Yu, Y. Hwa, J.-H. Kim and H.-J. Sohn, *J. Power Sources*, 2014, **260**, 174-179.
12. Y. Hwa, W.-S. Kim, B.-C. Yu, S.-H. Hong and H.-J. Sohn, *J. Phys. Chem. C*, 2013, **117**, 7013-7017.
13. H. Guo, H. Zhao, C. Yin and W. Qiu, *Mater. Sci. Eng., B*, 2006, **131**, 173-176.
14. Z. Zhang, Y. Wang, W. Ren, Q. Tan, Y. Chen, H. Li, Z. Zhong and F. Su, *Angew. Chem., Int. Ed.*, 2014, **53**, 5165-5169.
15. B.-C. Yu, Y. Hwa, J.-H. Kim and H.-J. Sohn, *Electrochim. Acta*, 2014, **117**, 426-430.
16. D. Chen, X. Mei, G. Ji, M. Lu, J. Xie, J. Lu and J. Y. Lee, *Angew. Chem., Int. Ed.*, 2012, **51**, 2409-2413, S2409/2401-S2409/2406.
17. G. Liu, S. Xun, N. Vukmirovic, X. Song, P. Olalde-Velasco, H. Zheng, V. S. Battaglia, L. Wang and W. Yang, *Adv. Mater. (Weinheim, Ger.)*, 2011, **23**, 4679-4683.
18. S. Zhou, X. Liu and D. Wang, *Nano Lett.*, 2010, **10**, 860-863.
19. B. Hertzberg, A. Alexeev and G. Yushin, *J. Am. Chem. Soc.*, 2010, **132**, 8548-8549.
20. X. Xin, X. Zhou, F. Wang, X. Yao, X. Xu, Y. Zhu and Z. Liu, *J. Mater. Chem.*, 2012, **22**, 7724-7730.
21. N. Dimov, S. Kugino and M. Yoshio, *Electrochim. Acta*, 2003, **48**, 1579-1587.
22. Y. He, X. Yu, Y. Wang, H. Li and X. Huang, *Adv. Mater. (Weinheim, Ger.)*, 2011, **23**, 4938-4941.
23. Y. Chen, S. Zeng, J. Qian, Y. Wang, Y. Cao, H. Yang and X. Ai, *ACS Appl. Mater. Interfaces*, 2014, **6**, 3508-3512.
24. N. Liu, H. Wu, M. T. McDowell, Y. Yao, C. Wang and Y. Cui, *Nano Lett.*, 2012, **12**, 3315-3321.
25. I. F. Perepichka, D. F. Perepichka, H. Meng and F. Wudl, *Adv. Mater.*, 2005, **17**, 2281-2305.
26. M. Yabushita, H. Kobayashi, K. Hara and A. Fukuoka, *Catal. Sci. Technol.*, 2014, **4**, 2312-2317.
27. P. Sun, S. Kuga, M. Wu and Y. Huang, *Cellulose (Dordrecht, Neth.)*, 2014, **21**, 2469-2478.
28. A. Sharif, J. Aalaie, H. Shariatpanahi, H. Hosseinkhanli and A. Khoshniyat, *J. Appl. Polym. Sci.*, 2013, **128**, 145-152.
29. M. Abareshi, S. M. Zebarjad and E. K. Goharshadi, *J. Compos. Mater.*, 2009, **43**, 2821-2830.
30. L. Zhang, L. Zhang, L. Chai, P. Xue, W. Hao and H. H. Zheng, *J. Mater. Chem. A*, 2014, DOI: 10.1039/C4TA04320K, Ahead of Print.
31. Z. Jiang, C. Li, S. Hao, K. Zhu and P. Zhang, *Electrochim. Acta*, 2014, **115**, 393-398.
32. X. H. Liu, Y. Liu, A. Kushima, S. Zhang, T. Zhu, J. Li and J. Y. Huang, *Adv. Energy Mater.*, 2012, **2**, 722-741.
33. J. Xie, G. Wang, Y. Huo, S. Zhang, G. Cao and X. Zhao, *Electrochim. Acta*, 2014, **135**, 94-100.
34. K. Fu, L. G. Xue, O. Yildiz, S. L. Li, H. Lee, Y. Li, G. J. Xu, L. Zhou, P. D. Bradford and X. W. Zhang, *Nano Energy*, 2013, **2**, 976-986.
35. L. Yue, W. Zhang, J. Yang and L. Zhang, *Electrochim. Acta*, 2014, **125**, 206-217.
36. K. J. Lee, S.-H. Yu, J.-J. Kim, D.-H. Lee, J. Park, S. S. Suh, J. S. Cho and Y.-E. Sung, *J. Power Sources*, 2014, **246**, 729-735.
37. D. M. Piper, T. A. Yersak, S.-B. Son, S. C. Kim, C. S. Kang, K. H. Oh, C. Ban, A. C. Dillon and S.-H. Lee, *Adv. Energy Mater.*, 2013, **3**, 697-702.
38. L. Zhu, Y. Niu, Y. Cao, A. Lei, X. Ai and H. Yang, *Electrochim. Acta*, 2012, **78**, 27-31.
39. R. Ruffo, S. S. Hong, C. K. Chan, R. A. Huggins and Y. Cui, *J. Phys. Chem. C*, 2009, **113**, 11390-11398.